ReMatch: Boosting Representation through Matching for Multimodal Retrieval

Qianying Liu^{1,2†*} Xiao Liang^{2*} Zhiqiang Zhang^{1‡} Zhongfei Qing Fengfan Zhou³ Yibo Chen² Xu Tang² Yao Hu² Paul Henderson^{2§}

¹University of Glasgow, Glasgow, UK ²Xiaohongshu Inc., Beijing, China ³Huazhong University of Science and Technology, Wuhan, China

https://github.com/FireRedTeam/ReMatch

Abstract

We present **ReMatch**, a framework that leverages the generative strength of MLLMs for multimodal retrieval. Previous approaches treated an MLLM as a simple encoder, ignoring its generative nature, and under-utilising its compositional reasoning and world knowledge. We instead train the embedding MLLM end-to-end with a chat-style generative matching stage. The matching stage uses the same MLLM to autoregressively decide relevance from multi-view inputs, including both raw data and its own projected embeddings for each query and document. It provides instancewise discrimination supervision that complements a standard contrastive loss, offering stronger gradients on hard negatives and preserving the compositional strengths of the original MLLM. To obtain semantically richer multimodal embeddings, we use multiple learnable tokens to augment each input, generating fine-grained contextual, mutually orthogonal embeddings with low inference cost. Leveraging our established high-performance baseline, we assemble the ideas mentioned above into a powerful training recipe and achieve a new state-of-the-art on the Massive Multimodal Embedding Benchmark (MMEB). Our experiments show particularly strong zero-shot generalization results on five datasets, highlighting the robustness and transferability of ReMatch.

1. Introduction

Multimodal embedding models are fundamental to image search [9], visual question answering [14, 48], and visual document retrieval [8]. These models embed heterogeneous inputs—such as images and text—into a shared representa-

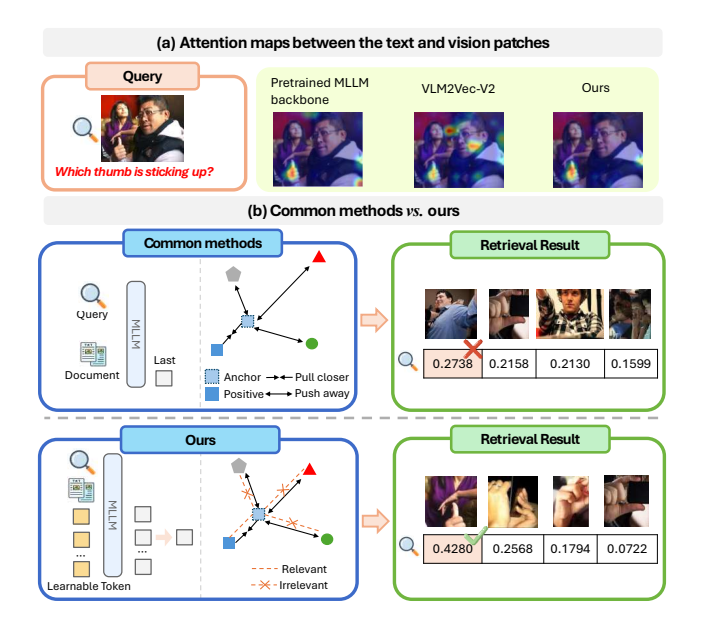


Figure 1. Illustration of our motivation. (a) Previous embedding methods like VLM2Vec-V2 disrupt the inherent fine-grained grounding of pretrained MLLMs. In contrast, our approach effectively preserves this critical alignment. (b) Our framework combines multiple learnable tokens with a generative matching objective to produce fine-grained and discriminative embeddings.

tion space, which allows us to solve tasks by finding matching embeddings between different modalities. Approaches like CLIP [32], BLIP [22] and SigLIP [45] show strong cross-modal retrieval performance, but still face limitations when inputs contain complex or highly varied instructions.

Recently, multi-modal large language models (MLLMs) have demonstrated strong potential for multimodal embedding, leveraging their native support for multimodal inputs [4, 7, 16, 24, 35, 49, 51]. Most existing approaches retain the causal-attention paradigm of native MLLMs; using

[†]Work was done during internship in Xiaohongshu Inc.

^{*}Equal contribution

[‡]Project lead

[§]Corresponding author (paul.henderson@glasgow.ac.uk)

specially designed prompts [16] they then extract embeddings from the last layer hidden state, typically corresponding to either the last token or a special [EOS] token. The extracted embeddings are then used for contrastive learning rather than next-token prediction.

Despite substantial progress in embedding MLLMs, recent work [52] shows that the final hidden state is optimized for generating vocabulary logits rather than preserving semantic structure, leading to suboptimal embeddings. Treating a MLLM as a single-vector embedding model without accounting for its autoregressive nature may reduce some of the pretrained backbone's abilities, such as integrating information across multimodal regions of interest (see top of Figure 1). We hypothesize this for two main reasons. Firstly, condensing the entire query and candidate into a single terminal vector (e.g. the hidden state of an [EOS] token) alters the model's original generative usage, where such tokens primarily serve logits-predict roles, and can not capture semantically rich representations in their hidden states [52]. Moreover a single vector is limited in capacity and cannot retain fine-grained details, particularly for highdimensional modalities such as images [42]. Secondly, relying solely on a global contrastive/discriminative loss may limit the preservation of its vision-language compositional understanding acquired during generative pretraining [31].

In this work, we propose *ReMatch* (**Representation** Enhanced via **Matching**), a novel approach to learning multimodal embeddings that leverages generative strengths of MLLMs. During training, it incorporates a chat-style matching stage ingesting the embeddings themselves, and a multi-token embedding strategy (see bottom of Figure 1).

Our first key contribution is to introduce a **chat-style matching mechanism that is applied when fine-tuning the MLLM for embedding**; this re-uses the same MLLM to autoregressively predict the relevance of multi-view input: both the raw data and embeddings of each query and document. This approach regularizes the MLLM and provides an stronger learning signal, encouraging its embeddings to capture finer semantic cues and allowing them to be fed back into the model for deeper understanding. It complements the standard InfoNCE contrastive objective, enhancing instance-wise image-text discrimination while preserving the compositional strengths of the original backbone. Furthermore, it provides stronger gradients for hard negatives, thereby mitigating negative-sampling bias.

As a second contribution, we introduce a small number of special learnable tokens appended to the input sequence of the query and candidate, whose last-layer hidden states serve as contextualized representations. This differs from the standard approach of encoding each query or candidate into one vector associated with the last token. To ensure these tokens capture complementary information and avoid collapsing into similar directions, we apply a soft

orthogonality loss.

To minimize the computational cost of multi-relevance decisions and late multi-token interaction [38], we first design a unified attention masking scheme that fully exploits the causal properties of MLLMs, enabling efficient multi-view matching within a single computation, and fuse multiple token embeddings into a single representation preserving diversity of information.

We consolidate training techniques into a reproducible plain baseline that nearly matches the current SOTA, establishing a new high-quality baseline that raises the bar for multimodal retrieval. On top of this enhanced baseline, our novel methods deliver further substantial gains and establish new SOTA performance on the MMEB benchmark.

2. Related Work

Multimodal Representation Embedding. CLIP [32] and subsequent models such as BLIP [22], CoCa [44], and SigLIP [45] have advanced vision-language pretraining by improving loss functions, data quality, and training strategies. However, most of these models still adopt a dual-encoder architecture, which constrains deeper crossmodal interactions. Recent studies have explored the use of MLLMs for multimodal representation learning [3, 10, 19, 31, 33]. For instance, E5-V [16] employs specially designed prompts to generate embeddings, while VLM2Vec [17] introduces a contrastive learning framework in conjunction with the Massive Multimodal Embedding Benchmark (MMEB). GME [49] further synthesizes fused-modal training data to enable universal multimodal retrieval. Other approaches enhance retrieval performance by generating large-scale synthetic datasets [4, 51] or leveraging hard negatives through advanced sampling strategies and gradient amplification [20, 35, 40]. MetaEmbed [38] adopts learnable tokens to produce compact multi-vector representations for fine-grained cross-modal matching. However, it uses a ColBERT-style [18] late-interaction paradigm, which introduces non-negligible computational overhead. In contrast, our approach retains the richness of multi-token embeddings while matching the computational efficiency of traditional single-vector methods.

Matching Module for Representation Learning. Early multimodal models such as ALBEF [21] and BLIP [22] introduce an image—text matching module to capture fine-grained vision—language alignments. In the MLLM era, matching is typically treated as an independent stage following retrieval [11, 27, 39], consistent with information retrieval paradigms. LamRA [27] introduces a two-stage framework where a separate reranker performs point-wise or list-wise reranking over results retrieved by LamRA-Ret to refine retrieval performance. UniME-V2 [11] leverages a MLLM as a judge to mine hard negatives for representa-

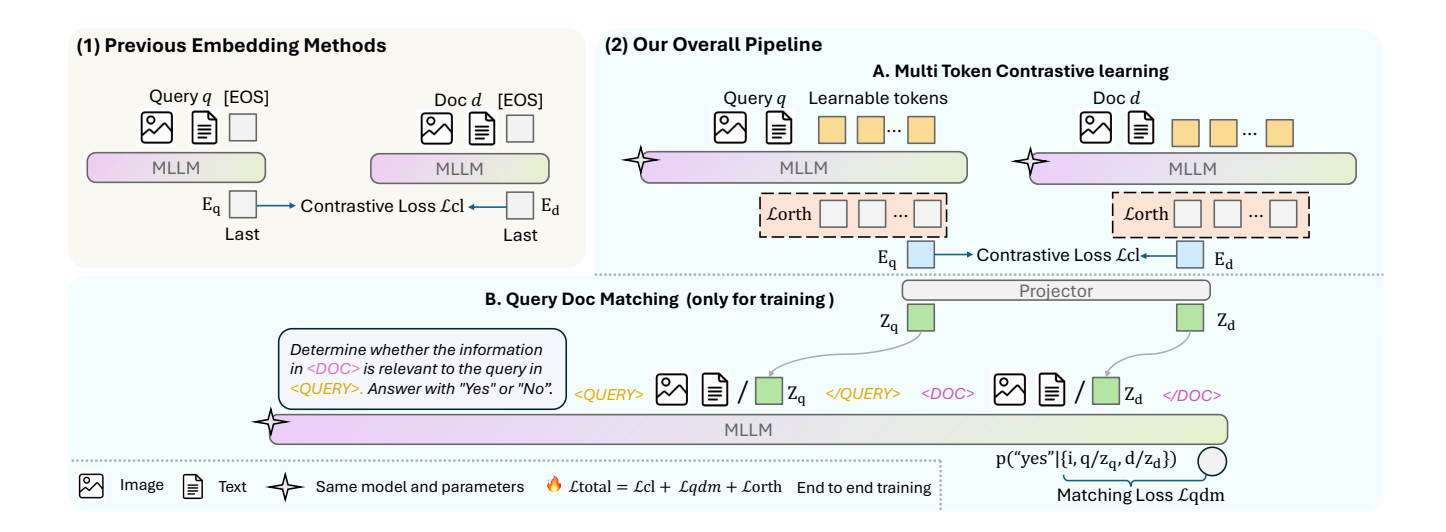


Figure 2. Previous multimodal retrieval frameworks v.s. our *ReMatch*. **Upper Left:** Single token retrieval method outputs an embedding for each pair of query and doc corresponding the [EOS] position, and uses contrastive objective to maximize the similarity for corresponding pairs. **Upper Right:** our framework first augments the input with Learnable Tokens and obtains multi-vector representations at these learnable-token positions. Then orthogonal regularization are employed on these representations and fuse into one embedding for every query or doc which are optimized by contrastive objective. The output embeddings are adapted by a MLP projector into MLLM input distribution, which used by our matching loss. **Lower:** we propose Query Doc Matching strategy to add point-wise discriminative signals in framework from original input and feature perspectives.

tion learning and to train a reranker with improved semantic discrimination. However, integrating such matching mechanisms into the MLLM paradigm to further enhance representation learning remains underexplored.

3. Method

We first (Sec. 3.1) revisit the definition of multimodal retrieval and outline our MLLM embedding baseline, discussing its key limitations that we aim to mitigate. We then present the ReMatch recipe (Sec. 3.2), and our main technical contributions (Sec. 3.2.1 and Sec. 3.2.3).

3.1. Preliminaries

Problem Definition. Multimodal retrieval involves retrieving relevant content across different modalities (e.g. text, image, video). We focus on text-image retrieval setting where the query q can be text (q_t) , an image (q_i) , or a combination of both (q_t, q_i) ; each candidate document d can similarly be any combination of text and image. Given a query q and a set of N candidate documents $\{d_1, d_2, \ldots, d_N\}$, a multimodal retrieval model defines the query embedding E(q) and document embeddings E(d), and then uses a similarity function s(E(q), E(d)) to measure the relevance between E(q) and E(d). The top-1 retrieved result d^* is then determined by:

$$d^* = \underset{d \in \{d_1, \dots, d_N\}}{\arg\max} s(E(q), E(d)). \tag{1}$$

Multimodal embedding large models. Recent retrieval methods project each modality to a shared embedding space via MLLM before measuring similarity. Concretely, state-of-the-art (SOTA) multimodal embedding models [4, 17, 49] are built on MLLMs with causal attention, typically appending an [EOS] token at the end of the input sequence. Given a multimodal input (query or document) x, where consists of both text tokens and image patches, and x then is tokenized into a representation $m = [m_1, \ldots, m_T]$. A decoder-only transformer produces a sequence of hidden states $f_{\theta}(x) = f_{\theta}(m; [EOS]) \in \mathbb{R}^{(T+1)\times d}$, where d is the hidden-state dimension and the j-th state only depends on $[m_1, \ldots, m_j]$. A natural choice for a single representation of x is derived from the hidden state of the last layer corresponding to this [EOS] token [49]: $E_{\theta}(x) := (f_{\theta}(x))_{T+1}$.

Discussion.

The above framework raises two key concerns: (i) Although separator tokens (e.g., ".", "\n" or [EOS]) are often associated with representations that aggregate contextual information [2], naively extracting their last-layer hidden states as representations may impair the inherent capability of MLLMs [31]. Moreover, a single token is may be insufficient to encode a large, compositional image—text input. (ii) Using only a contrastive loss optimises embedding distances globally, but may fail to capture finer correspondences between modalities [50]. Addressing these limitations is crucial for learning compact yet expressive representations that better capture fine-grained semantics

through richer contextualization. We next describe how Re-Match is designed to tackle the above issues.

3.2. Our design

We propose ReMatch, a framework that introduces chatstyle matching and learnable multi-token augmentation in an end-to-end fashion, designed to better activate and leverage the capabilities of the original MLLM for enhanced representation learning. (Fig. 2). To this end, each input is augmented with K learnable tokens (Sec. 3.2.1) whose directions are encouraged to be orthogonal. The resulting multi-token embeddings are fused and optimized by a contrastive loss (Sec. 3.2.2). Subsequently, the *raw* query—document pair *together with* their embeddings into the same MLLM with a chat-style prompt, and train it to output "Yes/No", providing instance-level discrimination supervision that complements the contrastive loss while preserving the compositional reasoning capabilities of the original MLLM (Sec. 3.2.3).

3.2.1. Multi Embedding Fusion

Learnable multi-token augmentation. To address the first issue in discussion, relying on the [EOS], we augment each input with $Learnable\ Tokens$ to better embed data, which are learned independently of the original MLLM vocabulary, ensuring their embeddings are decoupled from the model's generative outputs: $L_q \in \mathbb{R}^{K \times d}$ for queries and $L_d \in \mathbb{R}^{K \times d}$. The transformer then consumes $z^{(0)} = [m; L_q; L_d] \in \mathbb{R}^{(T+K+K) \times d}$, and produces last-layer hidden states $H = f_{\theta}(z^{(0)}) \in \mathbb{R}^{(T+K) \times d}$. We extract the final hidden states at these learnable-token positions to obtain a compact, contextualized multi-vector representation $ME_q = [e_1, \ldots, e_K] \in \mathbb{R}^{K \times d}$ and $ME_d \in \mathbb{R}^{K \times d}$, in two separate forward passes of the MLLM.

Orthogonal regularization. Since the K learnable tokens will later be fused into a single embedding and supervised by a contrastive loss, we would like these K token-level embeddings to carry non-overlapping information. We use a soft orthogonality constraint, replacing the hard constraint $e_i^\top e_j = 0$ with a differentiable penalty on pairwise inner products. Concretely, given the K learnable-token embeddings of E_q or $E_d = [e_1, \dots, e_K]$, we first L2-normalize them along the feature dimension $\tilde{e}_i = e_i/\|e_i\|_2$. We then penalize the embedding pairs if $i \neq j$:

$$\mathcal{L}_{\text{orth}} = \frac{2}{K(K-1)} \sum_{1 \le i < j \le K} (\tilde{e}_i^{\top} \tilde{e}_j)^2.$$
 (2)

In practice, we compute Eq. 2 for every sample in the batch and take the mean, encouraging the fused representation to aggregate diverse cues. After regularizing token diversity, we fuse the K token embeddings by simple averaging: $E_* = \frac{1}{K} \sum_{i=1}^K e_i \in \mathbb{R}^d$ where * denotes q or d, and use (E_q, E_d) in the contrastive loss introduced in the following.

3.2.2. Contrastive Fine-tuning

Each training instance is structured as a tuple $\mathcal{B}_i = (q_i, d_i^+, d_i^-)$, where q_i is the query, d_i^+ is its positive document, and d_i^- is explicit hard negative. Note that in contrastive learning, documents of other instances in the same batch, including both positive documents and negative documents, are also used as in-batch negatives, denoted by \mathcal{B} . Denote by E_{q_i} and E_d the final embeddings of the query and documents, respectively. The contrastive loss for \mathcal{B}_i is then defined as

$$\mathcal{L}_{cl}(\theta; \mathcal{B}_i) = -\log \frac{\Phi(E_{q_i}, E_{d_i^+})}{\Phi(E_{q_i}, E_{d_i^+}) + N},$$

$$N = \Phi(E_{q_i}, E_{d_i^-}) + \sum_{d \in \mathcal{B}} \Phi(E_{q_i}, E_d).$$
 (3)

where $\Phi(\cdot,\cdot)$ is a similarity function, e.g. $\Phi(a,b) = \exp(\cos(a,b)/\tau)$, with $\cos(\cdot,\cdot)$ the cosine similarity and τ a temperature.

3.2.3. Multi-View Query-Document Matching

Our MVQDM (Multi-View Query-Document Matching) strategy addresses the second challenge in the discussion of Sec. 3.1: improving fine-grained discriminative ability between samples. This strategy supplements InfoNCE [30] by injecting pointwise signals that drive absolute relevance judgments and deliver stronger gradients on hard negatives—mitigating negative-sampling bias.

Generative chat-style matching. Prior work (e.g., the BLIP series [22, 23]) feeds raw query–document pairs into the MLLM and applies an external binary classifier on its output. In contrast, we train the MLLM end-to-end to autoregressively generate a "Yes"/"No" token indicating query-document relevance directly from the paired inputs $(q,d^+/d^-)$. We optimize the supervised fine-tuning loss defined as:

$$\mathcal{L}_{\text{qdm}} = -\log p(l \mid P(\tilde{q}, \tilde{d})), \tag{4}$$

where $p(\cdot \mid *)$ is the probability assigned by the MLLM, and the label l is "Yes" for relevant d^+ and "No" for irrelevant d^- . \tilde{q} and \tilde{d} denote the query and document, which can be either raw data or projected embeddings (details are provided in the following section).

Multi-view input & efficiency. We design a multiview input scheme for the MLLM, leveraging both the raw data (q,d) and their embeddings (E_q,E_d) , as previously defined. Each embedding E_* is first transformed by a lightweight MLP: $Z_* = \text{MLP}(E_*)$, producing embeddings compatible with the input distribution of the same MLLM. The raw data and projected embeddings are then used by the MLLM to predict relevance. This encourages the model to capture both fine-grained signals from embeddings and

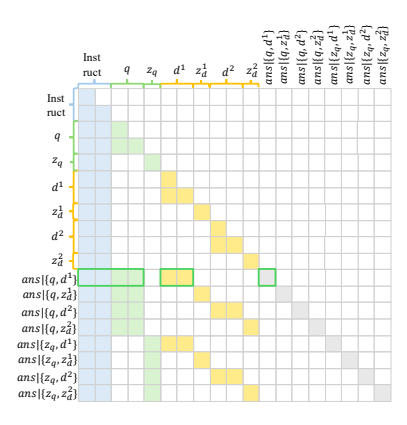


Figure 3. We introduce a unified attention mask that enables the model process all eight raw/embedding query–document combinations in one forward pass. Each answer token attends only to its paired query–document inputs (both raw and embedded) and the instruction prompt, preserving standard next-token prediction behavior. By randomizing which of d^1 , d^2 holds the d^+ , any positional leakage of relevance signals is prevented.

global contextual information from raw data, while keeping the entire computation within a single model instance.

To efficiently handle all eight possible query-document views without multiple MLLM forward passes, we employ a unified attention mask (Figure 3). Specifically, each query/document can be represented as raw data q/d or as projected embeddings Z_q/Z_d . For each training instance, we sample one positive document d^+ and one negative document d^- , yielding $\{q, Z_q\} \times (\{d^+, Z_{d^+}\} + \{d^-, Z_{d^-}\})$ (2×(2+2)=8 combinations). To avoid positional bias, we allocate the two document slots d^1, d^2 by randomly placing the positive document d^+ in one slot and the negative document d^- in the other. We then train the model to output "Yes" when d^+ is present and "No" otherwise.

Moreover, inspired by [31], we adopt a conversational template for the matching process. This mirrors the MLLM's generative pretraining regime, enabling us to fully leverage its pretrained generative capabilities. Overall the MLLM receives:

Prompt Template for Query-Document Matching: (Example shown for one query-document view.) USER: Compare the content inside <QUERY> and <DOC> . Determine whether the information in <DOC> is relevant to the query in <QUERY> . Answer only with "Yes" or "No". <QUERY>{query}/{query_feat}</QUERY> <DOC>{doc}/{doc_feat}</DOC> ASSISTANT: Yes/No

Lightweight alternative. To balance training complex-

ity and model performance, we propose an efficient alternative that takes only the token-level embeddings (z_q, z_d) as input—omitting the raw multimodal data. Experimental results in Sec. 4.3 demonstrate that this lightweight scheme still yields significant retrieval improvements.

3.2.4. Training Objectives

Our framework is trained end-to-end, jointly optimizing both the contrastive and matching tasks. The total loss combines the contrastive learning loss [30], orthogonality loss and query doc matching loss:

$$\mathcal{L} = \mathcal{L}_{cl} + w_{orth} \mathcal{L}_{orth} + w_{adm} \mathcal{L}_{adm}, \tag{5}$$

where w_{orth} and w_{qdm} are set to constant values of 0.5 and 0.1 respectively.

4. Experiments

Evaluation. To comprehensively evaluate the quality of method, we use the MMEB benchmark [17][28]. MMEB provides a comprehensive suite of 36 tasks to assess general multimodal capabilities, spanning four key areas: classification (CLS, 10 tasks), visual question answering (VQA, 10 tasks), retrieval (RET, 12 tasks), and visual grounding (VG, 4 tasks). Following the standard protocol, we report Hit@1 as the evaluation metric across all tasks. In addition, to rigorously evaluate the efficacy of ReMatch's unimodal embeddings, we benchmark its performance on five crossmodal retrieval tasks. These tasks encompass short-caption retrieval on Flickr30K [43] and COCO 2014 [26], long-caption retrieval on ShareGPT4V [5] and Urban1K [46], and compositional retrieval on SugarCrepe [12].

Implementation details. We train ReMatch on 8 NVIDIA H800 GPUs for 2500 steps with a global batch size of 1024 to ensure fair comparison with previous methods [29, 35]. All models are fine-tuned using LoRA [13] with r=32 and $\alpha=64$. We adopt a learning rate of 10^{-4} with a cosine decay schedule. The contrastive temperature is fixed at 0.02. Following [35, 41], we also introduce positive target prompts to disentangle different tasks, stabilizing the training. As for training dataset, we only incorporate MMEBtrain and one explicit hard negative from [4] for training all variants of ReMatch.

Models. To evaluate the effectiveness of ReMatch, we conduct experiments on various MLLMs of different sizes, including Qwen2-VL [36], and Qwen2.5-VL [1]. They represent unified multimodal architectures that process text and vision inputs. Our approach is benchmarked against a diverse set of baselines. These include dual-encoder frameworks like CLIP [32], UniLR [37], and MagicLens [47]. We also conduct direct comparisons with VLM2Vec-V1 [17] and VLM2Vec-V2[28], both of which leverage Qwen2-VL as their foundational MLLM. Furthermore, we assess

Table 1. Hit@1 (%) results on MMEB, which includes 36 tasks across four categories: Classification, Visual Question Answering (VQA), Retrieval, and Visual Grounding. IND and OOD represent the in-domain average and out-of-domain average metrics, respectively. **Bold** denotes the best scores in the subset and the second-best scores are highlighted with <u>underline</u>.

Model	Backbone	Size	P	er Meta	Average Score				
Wiodei	Dackbone	Size	Classification	VQA	Retrieval	Grounding	IND	OOD	Overall
CLIP [32]	ViT-L	428M	55.2	19.7	53.2	62.2	47.6	42.8	45.4
UniIR [37]	ViT-L14	428M	44.3	16.2	61.8	65.3	47.1	41.7	44.7
MagicLens [47]	ViT-L	613M	38.8	8.3	35.4	26.0	-	-	27.8
			MLLM-Based	Baseline	?S				
VLM2Vec [17]	Qwen2-VL	2B	59.0	49.4	65.4	73.4	66.0	52.6	59.3
VLM2Vec-V2 [29]	Qwen2-VL	2B	62.9	56.3	69.5	77.3	_	_	64.9
B3++ [35]	Qwen2-VL	2B	67.0	61.2	70.9	79.9	72.1	63.1	68.1
MoCa [3]	Qwen2.5-VL	3B	59.8	62.9	70.6	88.6	72.3	61.5	67.5
$\overline{\text{MM}}$ - $\overline{\text{EMBED}}$ [$\overline{25}$]	LLaVa-Next	$^{-}$ 7 $\bar{\mathrm{B}}$	48.1	32.2	63.8	57.8			50.0
GME [49]	Qwen2-VL	7B	56.9	41.2	67.8	53.4	-	_	55.8
VLM2Vec [17]	Qwen2-VL	7B	61.2	49.9	67.4	86.1	67.5	57.1	62.9
MMRet [51]	LLaVA-1.6 Mistral	7B	56.0	57.4	69.9	83.6	68.0	59.1	64.1
MoCa [3]	Qwen2.5-VL	7B	65.8	64.7	75.0	<u>92.4</u>	74.7	67.6	71.5
B3++ [35]	Qwen2-VL	7B	70.0	66.5	<u>74.1</u>	84.6	75.9	67.1	72.0
QQMM [40]	LLaVA-OneVision	7B	<u>69.9</u>	70.0	72.1	86.0	77.2	66.6	72.5
mmE5 [4]	Llama-3.2-Vision	11B	67.6	62.7	71.0	89.7	72.4	66.6	69.8
		Re	Match - Qwen2-	VL Initio	alized				
ReMatch	Qwen2-VL	2B	65.8	65.9	70.1	83.3	72.8	64.7	69.2
ReMatch	Qwen2-VL	7B	68.2	<u>71.8</u>	73.9	88.4	<u>77.4</u>	68.3	<u>73.3</u>
		Rel	Match - Qwen2.5	-VL Init	ialized				
ReMatch	Qwen2.5-VL	3B	62.4	69.6	70.0	92.0	75.1	64.0	70.2
ReMatch	Qwen2.5-VL	7B	65.8	73.6	<u>74.1</u>	92.5	78.1	<u>68.2</u>	73.7

performance against SOTA MLLM-based embedding techniques, such as MoCa [3], MMRet [51], MM-EMBED [25], GME [49], mmE5 [4], QQMM [40], and B3++ [35].

4.1. Comparison with Existing Methods

We report the overall multimodal embedding performance of different ReMatch variants and baseline methods on MMEB in Table 1. All ReMatch results are reported with 8 matching views and 16 learnable tokens; we measure the influence of these parameters in Sec. 4.3.

The encoder-based baselines are evaluated in a zero-shot setting, while the remaining models are trained on MMEB. ReMatch achieves the best results at comparable model sizes, outperforming the next best approach by 1.1% (B3++-2B), 2.7% (MoCa-3B), 1.2% (QQMM-7B). Compared to our baseline VLM2Vec, ReMatch achieves substantial improvements of 9.9% and 10.4%, respectively, on the 2B and 7B Qwen2-VL backbone. Notably, on the VQA task, our ReMatch models achieve substantial gains (+4.7% for the 2B groups and +3.6% for the 7B groups), as it more effectively uses the MLLM's latent world knowledge. The choice of backbone has a pronounced effect on ReMatch performance across tasks. ReMatch with Qwen2-VL

shows strong classification abilities (+3%), but its VQA and grounding score drops sharply, more than 3 and 8 points lower than the Qwen2.5-VL-initialized model. We notice that if the underlying base model itself struggles on some domains when used as a generative model, such a weakness directly propagates into ReMatch as an embedding model, similar to the findings in [15]. Moreover, ReMatch boosts retrieval quality without slowing down inference. Since relevance prediction occurs only during training, at test time ReMatch merely processes 16 additional tokens, incurring computational overhead comparable to VLM2Vec.

4.2. Zero-Shot Cross-Modal Retrieval on Short & Long Captions

We also evaluate ReMatch in a zero-shot setting across three kinds of retrieval benchmarks (short-caption; long-caption; compositional), underscoring the effectiveness of multi-token embedding paired with chat-style matching. As shown in Table 2, ReMatch-Qwen2-VL 2B delivers substantial gains over the strongest 2B-scale baseline (UniME-V2): +2.6% on text-to-image and +4.7% on image-to-text in Flickr30K, and +3.1%/ +11.4% on COCO. On long-caption tasks, ReMatch-2B exceeds UniME-V2 on Ur-

Table 2. Zero-shot text-image retrieval results (Recall@1) on short caption (Flickr30K, MS-COCO), long caption	(ShareGPT4V, Ur-
ban1K), and compositional (SugarCrepe) datasets.	

		Short Caption			Long Caption				Compositional			
Models	Size	Flickr30K		coco		ShareGPT4V		Urban1K		SugarCrepe		е
		$q^t \rightarrow c^i$	$q^i \rightarrow c^t$	Replace	Swap	Add						
OpenCLIP (ViT-L) [6]	0.4B	67.3	87.2	37.0	58.1	81.8	84.0	47.0	47.0	79.5	62.7	74.9
CLIP (ViT-BigG/14) [32]	2.5B	79.5	92.9	51.3	67.3	90.1	93.6	77.8	80.7	86.5	68.9	88.4
EVA-CLIP [34]	8B	80.3	94.5	52.0	70.1	93.1	91.2	80.4	77.8	85.9	70.3	86.7
VLM2Vec [17] (Qwen2-VL)	$\overline{2B}$	69.3	89.6	40.0	62.5	78.1	88.2	78.7	83.9	67.2	46.5	66.4
UniME [10] (Qwen2-VL)	2B	74.9	90.6	44.0	63.5	83.6	88.6	83.3	83.2	65.6	45.2	65.7
UniME-V2 [11] (Qwen2-VL)	2B	79.8	89.9	53.7	65.1	91.6	<u>94.2</u>	95.6	92.2	70.9	51.2	70.2
E5-V [16] (Phi3.5-V)	4.2B	72.2	79.6	44.7	53.4	86.0	88.5	83.8	83.6	88.2	66.6	75.3
Ē5-V [16] (LLaVĀ-1.6)	⁻ 7B ⁻	77.3	85.7	49.1	57.6	85.1	82.1	88.9	83.2	86.3	68.7	66.9
UniME [10] (Qwen2-VL)	7B	80.8	92.7	50.9	69.8	86.5	93.8	95.3	94.0	68.8	53.0	69.8
VLM2Vec [17] (Qwen2-VL)	7B	80.0	94.2	49.2	68.5	78.5	90.4	94.0	94.2	70.0	51.7	72.2
UniME [10] (LLaVA-OV)	7B	83.3	94.4	54.8	74.0	93.9	89.3	94.3	95.5	80.5	65.5	82.2
UniME-V2 [11] (Qwen2-VL)	7B	84.6	93.5	57.3	70.3	94.3	95.2	<u>97.2</u>	96.3	77.8	62.2	79.0
UniME-V2 [11] (LLaVA-OV)	7B	<u>85.5</u>	93.7	<u>60.9</u>	74.1	95.1	94.1	96.3	96.7	88.6	73.7	<u>90.5</u>
ReMatch - Qwen2-VL Initialized												
ReMatch (Qwen2-VL)	2B	82.4	<u>94.6</u>	56.8	<u>76.5</u>	93.3	92.4	96.0	<u>96.9</u>	90.3	73.8	90.3
ReMatch (Qwen2-VL)	7B	85.6	95.4	62.8	79.3	91.0	90.8	97.5	98.3	91.5	77.7	93.9

ban1K image-to-text by 4.7%, demonstrating its robustness to richer descriptions. Remarkably, on the SugarCrepe object-swap task, ReMatch-2B achieves +27.3% gain over VLM2Vec 2B. Scaling to 7B further boosts performance: ReMatch sets new bests on four of the five benchmarks (Flickr30K, COCO, Urban1K, SugarCrepe), and, notably, outperforms UniME-V2 with Qwen2-VL-7B (79.0%) by 14.9% on the attribution-adding subset of SugarCrepe.

4.3. Ablation Studies

We conduct various ablation experiments on different tasks within MMEB, using our ReMatch-2B (Qwen2-VL). We also show t-SNE visualization in the Appendix to compare the embedding distributions of our method and baselines.

Benefit of components. We first measure the benefit of each of the primary components of ReMatch; results are shown in Table 3. Our baseline (VLM2Vec) achieves 59.7% (top row). We first refine the training setup by tuning the parameters, adding task-specific target instructions and one explicit hard negative, yielding a strong tuning baseline that outperforms the original by 8.2%. Next, we evaluate our main contributions. First, our Multi-View Query-Document Matching (MVQDM) strategy alone lifts performance by 0.5%. To better align with the chat-style matching stage, we extend the embedding extraction with a chat-based prompt, denoted as MVQDM++, which improves over our tuning baseline by 1.1%. Furthermore, adding our Multi Embedding Fusion (MEF) alone brings a 0.8% improvement over tuning baseline. Lastly, combing all novel components yields the full model's SOTA performance (69.2%), demonstrating that both chat style

Table 3. Ablation study for the primary components of ReMatch 2B (Qwen2-VL). Training tuning: applies LoRA(rank=32, alpha=64), LR=1e-4 with cosine LR schedule, temperature=0.02 in CL loss on the baseline. MVQDM: multi-view query-document matching. MVQDM⁺⁺: further enhanced by incorporating a chatstyle template into the embedding extraction phase to align with matching. MEF: multi embedding fusion.

Ex	p Configuration	Overall	CLS	QA	RET	VG
0	Baseline (VLM2Vec)	59.7	58.7	49.3	65.0	72.9
	Our tun	ing variant				
1	Training Tuning	$65.5 \uparrow 5.8$	64.1	58.4	68.1	79.0
2	+ Target Instruction	$67.3 \uparrow 1.8$	65.0	63.2	68.3	80.6
3	+ Hard Negative Mining	$567.9 \uparrow 0.6$	65.0	64.8	69.0	80.2
	Our primar	y contribut	ions			
4	Exp3 + MVQDM	$68.4 \uparrow 0.5$	65.5	64.8	69.6	80.8
5	$Exp3 + MVQDM^{++}$	$68.8 \uparrow 0.9$	65.7	65.2	70.2	81.4
6	Exp3 + MEF	$68.7 \uparrow 0.8$	65.8	65.2	70.1	80.6
7	ReMatch-2B	69.2 ↑ 9.5	65.8	65.9	70.1	83.3

MVQDM and MEF are crucial for enhancing performance. **Effectiveness of matching.** To validate multi-view strategy in MVQDM, we compare five matching configurations in Table 5. "Raw \leftrightarrow Raw" uses the original query–document pair (q,d) as input, while "Feat \leftrightarrow Feat" uses their embedding pair (z^q,z^d) . Although any single view yields gains, the "Raw/Feat \leftrightarrow Raw/Feat" combination outperforms all others by a substantial margin (+0.5% over Exp3 in Table 3), demonstrating that multi-view matching delivers both finer-grained discrimination and a powerful regulariza-

Table 4. Effect of weight factor w_{qdm} for MVQDM loss.

t of weight	Table 5. Comparison of different
r MVQDM	matching views for MVQDM loss.

Overall

68.4

68.1

68.2

68.2

68.1

		Matching View
$w_{ m qdm}$	Overall	$Raw/Feat \leftrightarrow Raw/Feat$
0.1	68.4	$Feat \leftrightarrow Feat$
0.2	68.2	$Raw \leftrightarrow Raw$
0.4	68.0	$Raw \leftrightarrow Feat$
0.8	68.1	$Feat \leftrightarrow Raw$

Query	Rank1	Rank2	Rank3	Visualization
		Ours		
Select the portion of the image that answers the question "Which box frames the toilet?"		VLM2Vec		

Figure 4. Qualitative Comparison of Visual Grounding Results on the Visual7W-Pointing (OOD) Dataset.

tion effect. Notably, the Feat↔Feat view alone achieves performance nearly with Raw↔Raw (only 0.1% lower), providing a lightweight matching solution and confirming that ReMatch's projected embeddings are highly informative and could be readily understood by the same MLLM.

Table 4 reports the impact of the matching-loss weight $w_{\rm qdm}$ in Eq. (5). We sweep $w_{\rm qdm}$ from 0.1 to 0.8 and observe consistent gains of +0.2-+0.5% over the contrastive-only baseline (Exp3 in Table 3), confirming the robustness of our MVQDM strategy as an auxiliary loss. Notably, when combined with the chat template (Exp5 in Table 3), the matching yields up to a +0.9% gain, illustrating its strong synergy with the generative matching mechanism.

Qualitative results are shown in Figure 4. Given an input image and a question, we compare the top-3 retrieved regions and attention maps of the final layer produced by our method with MVQDM⁺⁺ (Exp5 in Table 3) and VLM2Vec-V2 (bottom row). Our method accurately retrieves the target patches, and the corresponding attention maps show focused activation on that interested object. This highlights a strong alignment between visual cues and the question semantics, demonstrating the fine-grained multimodal discriminative ability of our MVQDM⁺⁺.

Effectiveness of multi-token augmentation. Table 6 evaluates different token counts for our Multi Embedding Fusion (MEF). The first row corresponds to the single-vector baseline using only the [EOS] hidden state (Exp3 in



Figure 5. VQA retrieval Results on Place365 (OOD) and ScienceQA (OOD). Comparison between ours Exp6 and the baseline.

Table 6. Effect of multi-token (MT) fusion methods and number of tokens on Overall performance (%). OR: Orthogonal Multi-token Regularization.

MT Fuse Method	Num of tokens							
Will I age Wiewoa	1	4	8	16	32	64		
w/o MT ([EOS])	67.9	_	_	_	_			
Avg		68.6	68.4	68.4	68.2	68.5		
Avg + OR	_	68.3	68.3	68.7	68.7	68.8		

Table 3). Simply averaging K learnable tokens yields consistent but fluctuating gains across $K \in \{4, 8, 16, 32, 64\}$, peaking at +0.5%. When combined with our Orthogonal Multi-token Regularization (OR), the improvements become both larger and more stable, rising monotonically from +0.4% at K=4 to +0.9% at K=64, thereby demonstrating MEF's effectiveness and scalability.

To illustrate MEF's advantage in retaining pre-trained knowledge, Figure 5 presents two VQA cases. In Place365, our model (Exp 6) correctly retrieves the "science_museum" scene. In ScienceQA retrieval ("What is the capital of Mississippi?"), it retrieves "Jackson," whereas the [EOS]-based baseline fails. By distributing information across multiple learnable tokens rather than condensing into a single [EOS] vector, MEF preserves the MLLM's internal representations and better leverages its world knowledge. We also include in the appendix a visual comparison between average fusion and our orthogonal multi-token fusion, demonstrating the necessity of the orthogonality constraint.

5. Conclusion

We present ReMatch, a simple yet effective framework that unifies generative and discriminative representations in MLLMs for retrieval tasks. By introducing a chat-style generative matching strategy, Rematch embraces the autoregressive paradigm to deliver instance-level, multi-view relevance judgments while mitigating hard-negative bias. Moreover, we design learnable multi-token augmentation to produce fine-grained, mutually orthogonal embeddings, thereby better exploiting the MLLM's world knowledge. Extensive experiments show that our approach achieves SOTA on MMEB benchmark with remarkable zero-shot transfer across five retrieval tasks. ReMatch paves the way for a deeper unification of generative and discriminative paradigms in future multi-modal models.

References

- [1] Shuai Bai, Keqin Chen, Xuejing Liu, Jialin Wang, Wenbin Ge, Sibo Song, Kai Dang, Peng Wang, Shijie Wang, Jun Tang, Humen Zhong, Yuanzhi Zhu, Mingkun Yang, Zhaohai Li, Jianqiang Wan, Pengfei Wang, Wei Ding, Zheren Fu, Yiheng Xu, Jiabo Ye, Xi Zhang, Tianbao Xie, Zesen Cheng, Hang Zhang, Zhibo Yang, Haiyang Xu, and Junyang Lin. Qwen2.5-vl technical report, 2025.
- [2] Guoxuan Chen, Han Shi, Jiawei Li, Yihang Gao, Xiaozhe Ren, Yimeng Chen, Xin Jiang, Zhenguo Li, Weiyang Liu, and Chao Huang. Sepllm: Accelerate large language models by compressing one segment into one separator. *arXiv* preprint arXiv:2412.12094, 2024. 3
- [3] Haonan Chen, Hong Liu, Yuping Luo, Liang Wang, Nan Yang, Furu Wei, and Zhicheng Dou. Moca: Modality-aware continual pre-training makes better bidirectional multimodal embeddings. *arXiv* preprint arXiv:2506.23115, 2025. 2, 6
- [4] Haonan Chen, Liang Wang, Nan Yang, Yutao Zhu, Ziliang Zhao, Furu Wei, and Zhicheng Dou. mme5: Improving multimodal multilingual embeddings via high-quality synthetic data. *arXiv* preprint arXiv:2502.08468, 2025. 1, 2, 3, 5, 6
- [5] Lin Chen, Jinsong Li, Xiaoyi Dong, Pan Zhang, Conghui He, Jiaqi Wang, Feng Zhao, and Dahua Lin. Sharegpt4v: Improving large multi-modal models with better captions, 2023. 5
- [6] Mehdi Cherti, Romain Beaumont, Ross Wightman, Mitchell Wortsman, Gabriel Ilharco, Cade Gordon, Christoph Schuhmann, Ludwig Schmidt, and Jenia Jitsev. Reproducible scaling laws for contrastive language-image learning. In 2023 IEEE/CVF Conference on Computer Vision and Pattern Recognition (CVPR), page 2818–2829. IEEE, 2023. 7
- [7] Xuanming Cui, Jianpeng Cheng, Hong-you Chen, Satya Narayan Shukla, Abhijeet Awasthi, Xichen Pan, Chaitanya Ahuja, Shlok Kumar Mishra, Qi Guo, Ser-Nam Lim, et al. Think then embed: Generative context improves multimodal embedding. arXiv preprint arXiv:2510.05014, 2025. 1
- [8] Manuel Faysse, Hugues Sibille, Tony Wu, Bilel Omrani, Gautier Viaud, Céline Hudelot, and Pierre Colombo. Colpali: Efficient document retrieval with vision language models. arXiv preprint arXiv:2407.01449, 2024. 1
- [9] Albert Gordo, Jon Almazan, Jerome Revaud, and Diane Larlus. End-to-end learning of deep visual representations for image retrieval. *International Journal of Computer Vision*, 124(2):237–254, 2017. 1

- [10] Tiancheng Gu, Kaicheng Yang, Ziyong Feng, Xingjun Wang, Yanzhao Zhang, Dingkun Long, Yingda Chen, Weidong Cai, and Jiankang Deng. Breaking the modality barrier: Universal embedding learning with multimodal llms, 2025. 2, 7
- [11] Tiancheng Gu, Kaicheng Yang, Kaichen Zhang, Xiang An, Ziyong Feng, Yueyi Zhang, Weidong Cai, Jiankang Deng, and Lidong Bing. Unime-v2: Mllm-as-a-judge for universal multimodal embedding learning. arXiv preprint arXiv:2510.13515, 2025. 2, 7
- [12] Cheng-Yu Hsieh, Jieyu Zhang, Zixian Ma, Aniruddha Kembhavi, and Ranjay Krishna. Sugarcrepe: Fixing hackable benchmarks for vision-language compositionality, 2023. 5
- [13] Edward J Hu, Yelong Shen, Phillip Wallis, Zeyuan Allen-Zhu, Yuanzhi Li, Shean Wang, Lu Wang, Weizhu Chen, et al. Lora: Low-rank adaptation of large language models. *ICLR*, 1(2):3, 2022. 5
- [14] Hexiang Hu, Wei-Lun Chao, and Fei Sha. Learning answer embeddings for visual question answering. In *Proceedings* of the IEEE Conference on Computer Vision and Pattern Recognition, pages 5428–5436, 2018. 1
- [15] Chengyue Huang, Yuchen Zhu, Sichen Zhu, Jingyun Xiao, Moises Andrade, Shivang Chopra, and Zsolt Kira. Mimicking or reasoning: Rethinking multi-modal in-context learning in vision-language models. arXiv preprint arXiv:2506.07936, 2025. 6
- [16] Ting Jiang, Minghui Song, Zihan Zhang, Haizhen Huang, Weiwei Deng, Feng Sun, Qi Zhang, Deqing Wang, and Fuzhen Zhuang. E5-v: Universal embeddings with multimodal large language models. arXiv preprint arXiv:2407.12580, 2024. 1, 2, 7
- [17] Ziyan Jiang, Rui Meng, Xinyi Yang, Semih Yavuz, Yingbo Zhou, and Wenhu Chen. Vlm2vec: Training vision-language models for massive multimodal embedding tasks. *arXiv* preprint arXiv:2410.05160, 2024. 2, 3, 5, 6, 7
- [18] Omar Khattab and Matei Zaharia. Colbert: Efficient and effective passage search via contextualized late interaction over bert. In *Proceedings of the 43rd International ACM SI-GIR conference on research and development in Information Retrieval*, pages 39–48, 2020. 2
- [19] Fanheng Kong, Jingyuan Zhang, Yahui Liu, Hongzhi Zhang, Shi Feng, Xiaocui Yang, Daling Wang, Yu Tian, Fuzheng Zhang, Guorui Zhou, et al. Modality curation: Building universal embeddings for advanced multimodal information retrieval. arXiv preprint arXiv:2505.19650, 2025. 2
- [20] Zhibin Lan, Liqiang Niu, Fandong Meng, Jie Zhou, and Jinsong Su. Llave: Large language and vision embedding models with hardness-weighted contrastive learning. arXiv preprint arXiv:2503.04812, 2025. 2
- [21] Junnan Li, Ramprasaath Selvaraju, Akhilesh Gotmare, Shafiq Joty, Caiming Xiong, and Steven Chu Hong Hoi. Align before fuse: Vision and language representation learning with momentum distillation. Advances in neural information processing systems, 34:9694–9705, 2021. 2
- [22] Junnan Li, Dongxu Li, Caiming Xiong, and Steven Hoi. Blip: Bootstrapping language-image pre-training for unified vision-language understanding and generation. In *Interna*-

- tional conference on machine learning, pages 12888–12900. PMLR, 2022. 1, 2, 4
- [23] Junnan Li, Dongxu Li, Silvio Savarese, and Steven Hoi. Blip-2: Bootstrapping language-image pre-training with frozen image encoders and large language models. In *International conference on machine learning*, pages 19730–19742. PMLR, 2023. 4
- [24] Xiaojie Li, Chu Li, Shi-Zhe Chen, and Xi Chen. U-marvel: Unveiling key factors for universal multimodal retrieval via embedding learning with mllms. arXiv preprint arXiv:2507.14902, 2025. 1
- [25] Sheng-Chieh Lin, Chankyu Lee, Mohammad Shoeybi, Jimmy Lin, Bryan Catanzaro, and Wei Ping. Mm-embed: Universal multimodal retrieval with multimodal llms. arXiv preprint arXiv:2411.02571, 2024. 6
- [26] Tsung-Yi Lin, Michael Maire, Serge Belongie, Lubomir Bourdev, Ross Girshick, James Hays, Pietro Perona, Deva Ramanan, C. Lawrence Zitnick, and Piotr Dollár. Microsoft coco: Common objects in context, 2015. 5
- [27] Yikun Liu, Yajie Zhang, Jiayin Cai, Xiaolong Jiang, Yao Hu, Jiangchao Yao, Yanfeng Wang, and Weidi Xie. Lamra: Large multimodal model as your advanced retrieval assistant. In Proceedings of the Computer Vision and Pattern Recognition Conference, pages 4015–4025, 2025. 2
- [28] Rui Meng, Ziyan Jiang, Ye Liu, Mingyi Su, Xinyi Yang, Yuepeng Fu, Can Qin, Zeyuan Chen, Ran Xu, Caiming Xiong, Yingbo Zhou, Wenhu Chen, and Semih Yavuz. Vlm2vec-v2: Advancing multimodal embedding for videos, images, and visual documents, 2025. 5
- [29] Rui Meng, Ziyan Jiang, Ye Liu, Mingyi Su, Xinyi Yang, Yuepeng Fu, Can Qin, Zeyuan Chen, Ran Xu, Caiming Xiong, et al. Vlm2vec-v2: Advancing multimodal embedding for videos, images, and visual documents. arXiv preprint arXiv:2507.04590, 2025. 5, 6
- [30] Aaron van den Oord, Yazhe Li, and Oriol Vinyals. Representation learning with contrastive predictive coding. *arXiv* preprint arXiv:1807.03748, 2018. 4, 5
- [31] Yassine Ouali, Adrian Bulat, Alexandros Xenos, Anestis Zaganidis, Ioannis Maniadis Metaxas, Brais Martinez, and Georgios Tzimiropoulos. Vladva: Discriminative fine-tuning of lvlms. In *Proceedings of the Computer Vision and Pattern Recognition Conference*, pages 4101–4111, 2025. 2, 3, 5
- [32] Alec Radford, Jong Wook Kim, Chris Hallacy, Aditya Ramesh, Gabriel Goh, Sandhini Agarwal, Girish Sastry, Amanda Askell, Pamela Mishkin, Jack Clark, et al. Learning transferable visual models from natural language supervision. In *International conference on machine learning*, pages 8748–8763. PmLR, 2021. 1, 2, 5, 6, 7
- [33] JungKyoo Shin, Bumsoo Kim, and Eunwoo Kim. Generative modeling of class probability for multi-modal representation learning. In *Proceedings of the Computer Vision and Pattern Recognition Conference*, pages 20737–20746, 2025. 2
- [34] Quan Sun, Yuxin Fang, Ledell Wu, Xinlong Wang, and Yue Cao. Eva-clip: Improved training techniques for clip at scale. *arXiv preprint arXiv:2303.15389*, 2023. 7
- [35] Raghuveer Thirukovalluru, Rui Meng, Ye Liu, Mingyi Su, Ping Nie, Semih Yavuz, Yingbo Zhou, Wenhu Chen,

- Bhuwan Dhingra, et al. Breaking the batch barrier (b3) of contrastive learning via smart batch mining. *arXiv preprint arXiv:2505.11293*, 2025. 1, 2, 5, 6
- [36] Peng Wang, Shuai Bai, Sinan Tan, Shijie Wang, Zhihao Fan, Jinze Bai, Keqin Chen, Xuejing Liu, Jialin Wang, Wenbin Ge, Yang Fan, Kai Dang, Mengfei Du, Xuancheng Ren, Rui Men, Dayiheng Liu, Chang Zhou, Jingren Zhou, and Junyang Lin. Qwen2-vl: Enhancing vision-language model's perception of the world at any resolution, 2024. 5
- [37] Cong Wei, Yang Chen, Haonan Chen, Hexiang Hu, Ge Zhang, Jie Fu, Alan Ritter, and Wenhu Chen. Uniir: Training and benchmarking universal multimodal information retrievers. In *European Conference on Computer Vision*, pages 387–404. Springer, 2024. 5, 6
- [38] Zilin Xiao, Qi Ma, Mengting Gu, Chun-cheng Jason Chen, Xintao Chen, Vicente Ordonez, and Vijai Mohan. Metaembed: Scaling multimodal retrieval at test-time with flexible late interaction. *arXiv* preprint arXiv:2509.18095, 2025. 2
- [39] Mingjun Xu, Jinhan Dong, Jue Hou, Zehui Wang, Sihang Li, Zhifeng Gao, Renxin Zhong, and Hengxing Cai. Mm-r5: Multimodal reasoning-enhanced reranker via reinforcement learning for document retrieval. arXiv preprint arXiv:2506.12364, 2025. 2
- [40] Youze Xue, Dian Li, and Gang Liu. Improve multi-modal embedding learning via explicit hard negative gradient amplifying, 2025. 2, 6
- [41] Youze Xue, Dian Li, and Gang Liu. Improve multi-modal embedding learning via explicit hard negative gradient amplifying. *arXiv preprint arXiv:2506.02020*, 2025. 5
- [42] Lewei Yao, Runhui Huang, Lu Hou, Guansong Lu, Minzhe Niu, Hang Xu, Xiaodan Liang, Zhenguo Li, Xin Jiang, and Chunjing Xu. Filip: Fine-grained interactive language-image pre-training. *arXiv preprint arXiv:2111.07783*, 2021. 2
- [43] Peter Young, Alice Lai, Micah Hodosh, and Julia Hockenmaier. From image descriptions to visual denotations: New similarity metrics for semantic inference over event descriptions. *Transactions of the Association for Computational Linguistics*, 2:67–78, 2014. 5
- [44] Jiahui Yu, Zirui Wang, Vijay Vasudevan, Legg Yeung, Mojtaba Seyedhosseini, and Yonghui Wu. Coca: Contrastive captioners are image-text foundation models. arXiv preprint arXiv:2205.01917, 2022. 2
- [45] Xiaohua Zhai, Basil Mustafa, Alexander Kolesnikov, and Lucas Beyer. Sigmoid loss for language image pre-training. In Proceedings of the IEEE/CVF international conference on computer vision, pages 11975–11986, 2023. 1, 2
- [46] Beichen Zhang, Pan Zhang, Xiaoyi Dong, Yuhang Zang, and Jiaqi Wang. Long-clip: Unlocking the long-text capability of clip, 2024. 5
- [47] Kai Zhang, Yi Luan, Hexiang Hu, Kenton Lee, Siyuan Qiao, Wenhu Chen, Yu Su, and Ming-Wei Chang. Magiclens: Self-supervised image retrieval with open-ended instructions. *arXiv preprint arXiv:2403.19651*, 2024. 5, 6
- [48] Sheng Zhang, Min Chen, Jincai Chen, Fuhao Zou, Yuan-Fang Li, and Ping Lu. Multimodal feature-wise co-attention method for visual question answering. *Information Fusion*, 73:1–10, 2021. 1

- [49] Xin Zhang, Yanzhao Zhang, Wen Xie, Mingxin Li, Ziqi Dai, Dingkun Long, Pengjun Xie, Meishan Zhang, Wenjie Li, and Min Zhang. Gme: Improving universal multimodal retrieval by multimodal llms. *CoRR*, 2024. 1, 2, 3, 6
- [50] Yiwu Zhong, Jianwei Yang, Pengchuan Zhang, Chunyuan Li, Noel Codella, Liunian Harold Li, Luowei Zhou, Xiyang Dai, Lu Yuan, Yin Li, et al. Regionclip: Region-based language-image pretraining. In *Proceedings of the IEEE/CVF conference on computer vision and pattern recognition*, pages 16793–16803, 2022. 3
- [51] Junjie Zhou, Yongping Xiong, Zheng Liu, Ze Liu, Shitao Xiao, Yueze Wang, Bo Zhao, Chen Jason Zhang, and Defu Lian. Megapairs: Massive data synthesis for universal multimodal retrieval. In *Proceedings of the 63rd Annual Meeting of the Association for Computational Linguistics (Volume 1: Long Papers)*, pages 19076–19095, 2025. 1, 2, 6
- [52] Yuhan Zhu, Xiangyu Zeng, Chenting Wang, Xinhao Li, Yicheng Xu, Ziang Yan, Yi Wang, and Limin Wang. Freeret: Mllms as training-free retrievers. *arXiv preprint* arXiv:2509.24621, 2025. 2

ReMatch: Boosting Representation through Matching for Multimodal Retrieval

Supplementary Material

S6. Embedding Distribution Visualization

We first assess whether queries and documents are semantically aligned, i.e., embedded in close proximity without domain shift. Figure 6 presents t-SNE visualizations of query-document embeddings on the MMEB benchmark, comparing the baseline VLM2Vec-V2 with our ReMatch. For each of the four tasks, we randomly sample three different subtasks. On all settings, ReMatch yields substantially tighter clustering between matched queries and documents than VLM2Vec-V2, reflecting its improved embedding alignment. Notably, on the VQA and retrieval tasks, VLM2Vec-V2 produces two clearly separated clusters, one with queries and the other with documents; in contrast Re-Match achieves a great increase in distribution overlap.

S7. Full Prompt for MVQDM

This is our full prompt template for MVQDM with eight views. Due to space limits in the main text, we only present a simplified version in Sec. 3.2.3.

Prompt Template for MVQDM with Eight Views: SYSTEM: You are a helpful assistant. USER: Compare the content inside <QUERY> and <DOC>. Determine whether the information in <DOC> is relevant to the query in <QUERY>. Answer only with "Yes" or "No", and wrap your answer in <ANSWER></ANSWER> tags. <QUERY> {query} </QUERY> <QUERY> <feat_start> {query_feat} <feat_end> </QUERY> <DOC> {doc1} </DOC> <DOC> <feat_start> {doc1_feat} <feat_end> </DOC> <DOC> {doc2} </DOC> <DOC> <feat_start> {doc2_feat} <feat_end> </DOC> ASISTANT: <ANSWER>{ans1}</ANSWER> <ANSWER>{ans1}</ANSWER> <ANSWER>{ans2}</ANSWER> <ANSWER>{ans2}</ANSWER> <ANSWER>{ans1}</ANSWER> <ANSWER>{ans1}</ANSWER> <ANSWER>{ans2}</ANSWER> <ANSWER>{ans2}</ANSWER>

Moreover, we introduce MVQDM⁺⁺, which embeds the inputs within a chat-style template to fully align with the matching paradigm. By contrast, previous methods, such as VLM2Vec-V2 or B3, derive embeddings from inputs of the

form: {image} {text} {task instruction}.

```
Embedding Prompt Template for MVQDM**:

SYSTEM: You are a helpful assistant.

USER:{image} {text} {task instruction}

ASSISTANT:
```

S8. Effectiveness of orthogonal regularization in multi-embedding fusion.

To produce the attention visualizations in Figures 1, 4 and 7, we extract the MLLM's last layer (28th of Qwen-VL-2B) attention weights between each embedding token (VLM2Vec-V2 uses last token; our method includes all learnable tokens) and the image patches. For each token, we average the attention weights across heads, apply a min-max normalization to [0,1], and reshape it into the original patch-grid dimensions. We then overlay this attention map onto the RGB input. Side by side, these overlays reveal the different regions each token focuses on, showing the richer, more diverse semantics of our multi-token representations.

Figure 7 validates our key hypothesis: simply appending multiple learnable tokens (MEF + Avg) often yields highly redundant information across tokens. Each token attends to the same image regions, thus increasing the token count alone does not improve performance. By contrast, adding our soft orthogonal regularization (MEF + Avg + OR) forces each token to specialize on different parts of the scene, enriching the overall embedding. Specifically, in case (a), only the OR-regularized model correctly grounds the appliance that the toddler is standing in front of the oven; in case (b), the regularized version attends separately to the upper and lower tree clusters and correctly classifies the scene as a "vegetable garden," whereas the unregularized maps collapse onto the lower foliage and misclassify it; and in case (c), the attention maps without OR look virtually identical and still miss large portions of the riverbank, whereas our OR-enhanced tokens collectively cover the full watercourse and recover the correct grounding.

S9. Beyond Embeddings: Can Embedding MLLMs Still Speak Fluently?

As discussed above, multimodal embedding models disregard the backbone's autoregressive nature. They improve discriminative ability via contrastive learning but may attenuate the backbone's world knowledge and generative capacity. This prompts the question: after contrastive finetuning, can these embedding models still preserve image-

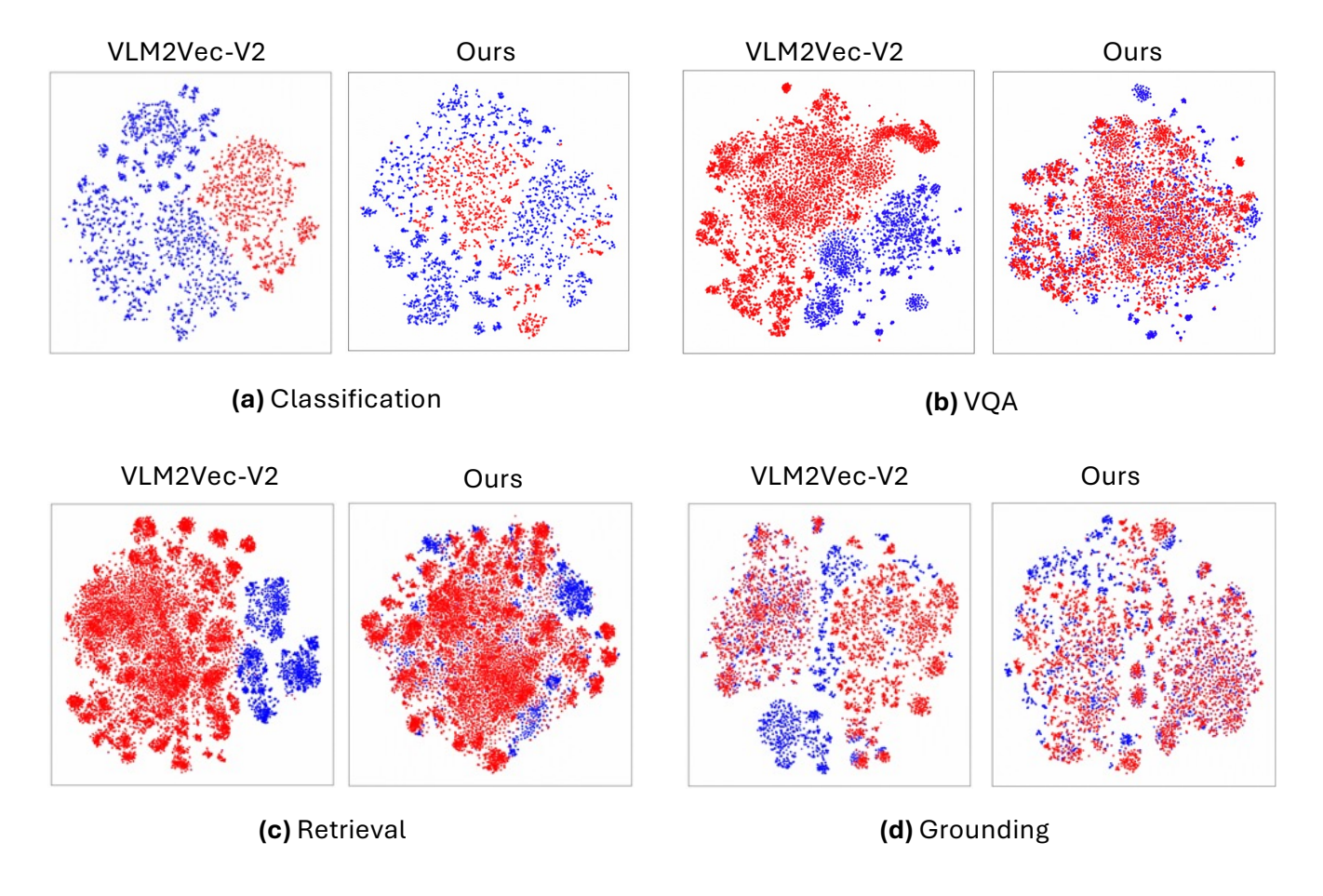


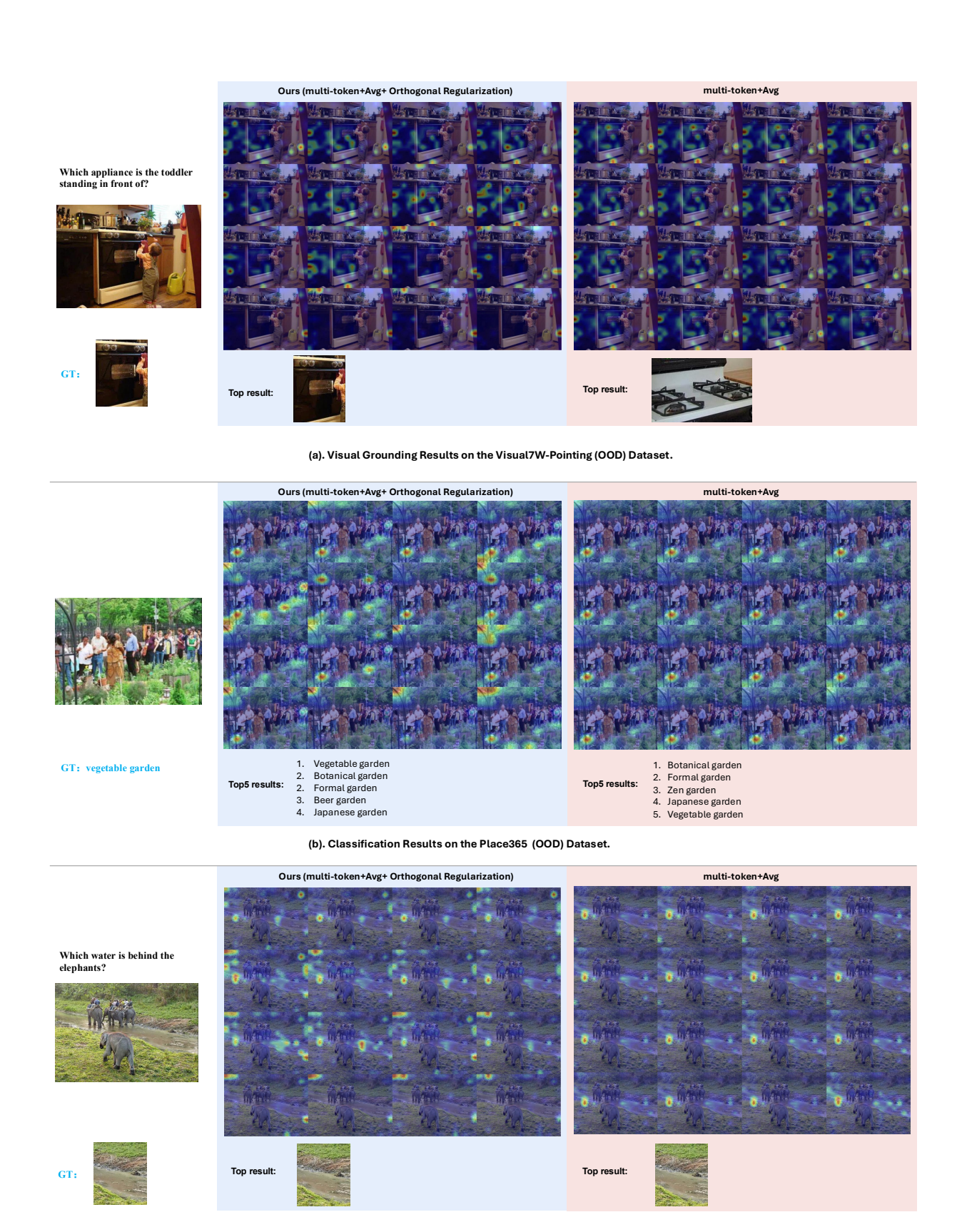
Figure 6. t-SNE (perplexity = 30) of query and document embeddings on four tasks, comparing VLM2Vec-V2 2B (left) with our Re-Match 2B (Qwen2-VL, right). Desired geometry is tight query-document co-localization in compact, overlapping clusters. Conversely, pronounced red-blue segregation or large single-color regions indicate weak query-document alignment and degraded embedding quality. Best viewed with zoom.

captioning performance? Here, unlike elsewhere in the paper, the MLLM generates text autoregressively, conditioned on the image provided in its prompt. Figure 8 and 9 present results on three long-caption and two short-caption cases, comparing the original backbone (Qwen2-VL-2B) with two representative embedding methods— GME (compresses features into [EOS]) and VLM2Vec-V2 (uses the last token). Across all five examples, both baselines fail to produce fluent descriptions, frequently exhibiting repetition and VLM2Vec-V2 even shows mixed-language outputs (e.g., Chinese and Thai). In contrast, ReMatch nearly seamlessly retains the comparable generation quality of Qwen2-VL-2B. This finding indicates that single-token embedding compression at [EOS] or at the last token degrades the backbone's autoregressive generation ability. By contrast, a learnable multi-token enhancement combined with a chat style matching strategy not only substantially improves embedding performance but also preserves the model's generative capacity.

S10. More Visualization for four tasks on MMEB

In this section, we present additional visual comparisons between our method and VLM2Vec-V2 on the MMEB benchmark (Figures 10–13). For each of four tasks (classification, VQA, retrieval, and visual grounding), we report two cases. In the resulting eight examples, our method shows consistently superior performance.

Note. In the main text, we use VLM2Vec as our baseline (the starting point for ReMatch), while in the appendix we compare against a stronger variant, VLM2Vec-V2, to further emphasize our performance gains.



(c). Visual Grounding Results on the Visual7W-Pointing (OOD) Dataset.

Figure 7. Attention maps between the query image and each learnable token (16 tokens; 4×4 grid) and retrieval results of our method, with and without orthogonal regularization in MEF, across three cases.

Give a detailed description of the image. Owen2-VL-Instruct:



The image depicts a equestrian event, specifically a show jumping competition. The scene is set in an outdoor arena with a sandy ground, and the background features a row of buildings and a few trees. The main focus is on a horse and rider in mid-jump over a colorful, multi-colored hurdle. The horse is a grey with white patches, and it appears to be in mid-air, with its front legs raised and its hind legs bent, indicating a dynamic and controlled jump. The rider is dressed in a black riding suit, white pants, and black boots, and is aring a black helmet. The rider\'s posture is upright, suggesting they are experienced and focused on the task at hand.

The hurdle is made of metal and has a variety of colors, including red, blue, yellow, and green, arranged in a diagonal pattern. The rider is holding the reins with both hands, and the horse\'s head is slightly tilted, showing concentration and effort. The background includes a digital timer displaying "1.00," which likely indicates the time elapsed since the horse cleared the hurdle

In the foreground, there are several white barriers with colorful signs and banners, possibly indicating the names of sponsors or sponsors\ logos. The arena is enclosed by white tents, and there are spectators seated on chairs, watching the event. The spectators are dressed casually, suggesting this is a public event rather than a professional one.

The overall atmosphere of the image is one of excitement and concentration, capturing the essence of equestrian sport. The image does not contain any text or additional objects that are not visible in the provided description

person on horseback in mid-air over an obstacle course bar. Equestrian sport, jumping over an obstacle course bar. Equestrian sport, jumping over an obstacle course bar. Equestrian sport, jumping over an obstacle course bar..

VLM2Vec-V2:

跳跃比赛正在进行。灰色或多样的马匹,跳跃越过七七栏。灰色马跳跃越过七七栏,七七栏上有七七数字,七七七七七七七七七七

ReMatch:

The image depicts an equestrian event, specifically a horse jumping over an obstacle. The horse is a grey and white speckled breed, with a black mane and tail. It is equipped with a saddle and a saddle blanket that is purple and brown in color. The rider is dressed in a black helmet, a black jacket, white pants, and black boots. The rider\'s posture is focused and determined, indicating a high level of skill and experience. The obstacle is a colorful, multi-barred structure made of wood and metal, painted in red, blue, yellow, and white. The rider is positioned on the left side of the structure, with the horse\'s body leaning forward as it leaps over the last bar. The horse\'s front right leg is lifted off the ground, while the left front leg is still on the ground, providing balance.

In the background, there are several white tents set up, likely for the event, with one prominently displaying the word "Habor" in both English and Chinese characters. Additionally, there is a large digital display showing the score of 1.00, indicating that the event is likely a competition or a high-level event. The ground is a dirt track, and the overall setting suggests a well-organized and professiona environment.

The image captures a moment of intense concentration and athleticism, highlighting the bond between the horse and its rider as they navigate the obstacle together. The rider\'s posture and the horse\'s form suggest that this is a well-trained and experienced pair, possibly preparing for a larger competition or a high-level event.

Overall, the image is a dynamic and detailed portrayal of equestrian performance, emphasizing the rider\'s skill and the horse\'s ability to execute a jump with precision and grace.

Provide an in-depth description of the



Owen2-VL-Instruct:

The image depicts a serene mountainous landscape during what appears to be either sunrise or sunset, given the warm, golden hues in the sky. The foreground is dominated by a tall, dark tree with a thick trunk and a dense canopy of needles. The tree's silhou ette is stark against the lighter background, creating a striking contrast.

Beyond the tree, the landscape is filled with rolling hills and valleys, covered in lush greenery. The hills are slightly hilly, with some areas appearing more rugged and rocky. The valleys are wide and deep, with gentle slopes that gently curve into the distance. The sky above is clear, with a gradient of colors ranging from a light blue at the top to a deeper blue and then to a warm orange near the horizon. The sunlight casts long shadows, adding depth and dimension to the scene.

The overall atmosphere of the image is calm and peaceful, with the natural beauty of the mountains and trees creating a sense of tranquility. The lighting suggests that the sun is low in the sky, casting long shadows and creating a warm, golden light that enhances the

GME:

Image Description: Pine tree trunk and branches, mountains, hills, valleys, and valleys. Image Location: Image location: Image location: Image location: Image location: Image location:

VI M2Vec-V2:

The image depicts a serene and expansive mountainous landscape during what appears to be either sunrise or sunset, given the warm, golden hue filtering through the tree branches. The tree in the foreground is a tall, dark pine or similar conifer, its trunk prominently featured against the backdrop of the surrounding mountains. The tree's branches extend outward, casting intricate shadows on the surrounding foliage and the lower parts of the mountainside.

The tree is situated in a valley or a depression, which is illuminated by the soft, diffused light filtering through the tree branches. The valley is characterized by a series of gentle hills and ridges, each with varying shades of green, indicating a mix of different types of vegetation. The tree itself is silhouetted against the lighter, more distant mountains, which are bathed in a warm, golden light that

As the tree branches extend outward, they create a natural archway, framing the tree and the valley below. The branches are densely packed with needle-like, needle-like leaves, which are primarily dark green with some lighter green tips. The tree appears to be a dominant feature in the image, its size and prominence making it a focal point against the softer, more distant landscape

In the background, the tree is set against a range of mountains that continue into the distance, their peaks partially obscured by the warm light filtering through the tree branches. The mountains are layered, with each successive range appearing darker and more defined as they recede into the distance. The overall scene is one of tranquility and natural beauty, with the warm light and the dark, silhouetted tree creating a contrast that highlights the depth and scale of the landscape.

The image does not contain any discernible text or human-made structures, focusing solely on the natural elements of the environment. The absence of any specific landmarks or identifiable features further emphasizes the vastness and untouched quality of the scene

In summary, the image is a tree in the foreground of a valley, with warm, golden light filtering through the tree branches, casting a natural archway over the valley below. The tree is a dark, tall conifer, surrounded by a series of hills and valleys illuminated by the warm, golden light of the setting or rising sun. The image evokes a sense of peace and the vastness of nature.

Figure 8. Comparison of image captioning performance between our method, original backbone and prior embedding approaches (all based on Qwen2-VL-2B). Part 1.

Write a detailed explanation of what the image shows.



Qwen2-VL-Instruct:

The image depicts two dogs playing in an outdoor setting. The background features a wire fence, suggesting that the scene is taking place in a fenced area, possibly a farm or a rural field. The ground is covered with dry grass and dirt, indicating that it might be late autumn or winter.

The black dog, which appears to be a Labrador Retriever, is standing on its hind legs and appears to be jumping or leaping towards the white dog. The white dog, which is a German Shepherd, is lying on its back on the ground, with its front paws raised and its head turned towards the black dog. The black dog's expression seems to be playful or excited, while the white dog's expression is more relaxed and content.

The overall scene is lively and suggests a moment of interaction between the two dogs, possibly engaging in a playful or interactive activity. The dry grass and the wire fence add to the rural and natural setting, emphasizing the outdoor environment.

GME:

Image description: Black labrador black labrador and white German Shepherd white German shepherd play together on dry grass. Black labrador black labrador and white German Shepherd white German shepherd play together on dry grass. Black labrador Black labrador and white German Shepherd Play together on dry grass. Black labrador and white German Shepherd play together on dry grass. Black labrador Black labrador and white German Shepherd play together on dry grass......

VLM2Vec-V2:

Black dog Black dog

ReMatch

The image depicts two dogs engaging in a playful interaction on a dirt field with a wire fence in the background. The black dog, which is a German Shepherd. The black dog is oriented towards the white dog, and it has a focused expression, possibly indicating that it is about to land on the white dog. The white dog is lying on its back on the ground, with its front paws raised and its body stretched out, appearing to be in a submissive or playful position. The black dog's collar is visible, and it has a collar with a blue band. The white dog's fur is predominantly white, with a black nose and a small brown spot on its forehead. The overall scene is one of dynamic movement and interaction between the two dogs. The background includes a wire mesh fence that separates the field from a road or a similar structure. The lighting suggests that the photo was taken during the evening or at dusk, as the sky is not fully visible but the overall ambiance is warm and soft.

Describe the image briefly.



Owen2-VL-Instruct:

The image depicts a marina with various boats docked. There are lifeboats, sailboats, and other vessels, all reflecting in the calm water. The background features a row of red-brick buildings, possibly residential or commercial, with a clear blue sky above. The scene is serene and picturesque, capturing the essence of a peaceful harbor.

GME:

Blue sky, blue water, red brick buildings, orange lifeboat, blue boat with blue flag, red and white sailboat, blue and white sailboat, red brick building, red brick building, red brick building, red brick building, red brick building.....

VLM2Vec-V2

橙色 lifeboat, blue lifeboat, blue sailboat, blue sailboat with blue flag, blue lifeboat, blue sailboat with blue flag, blue lifeboat......

ReMatch:

The image features a marina with various types of boats docked. In the foreground, there is a blue and orange lifeboat, a blue sailboat with a blue flag, and other smaller boats. The background includes a large red brick building with a blue sky and clouds above. The water is calm, and the reflection of the boats can be seen on the surface.

Give a short description of the picture.



Qwen2-VL-Instruct:

The image shows a display of decorative items in a store. There are two large table lamps with beige lampshades, one with a rustic wooden base and the other with a more modern design. In front of the lamps, there is a vase with pink flowers and a small bowl. To the right of the lamps, there are three decorative jars with intricate designs, one of which is blue and the others are white. Additionally, there are two small wooden containers and a stack of books on the table. In the background, there is a large painting of a cityscape with boats and people. The store is called "adjectives."

GMF.

Lamps, vases, and other items on table top with flowers and books. Lamps with beige shades, vases with flowers, books, and other items on table top with flowers and books. Lamps with beige shades, vases with flowers, books, and other items on table top with flowers and books. Lamps with beige shades, vases with flowers, books, and other items on table top with flowers and books......

VLM2Vec-V2

ևտոս lamps with flowers and lanterns on table with lampshades and tableware. Adjectives Adjective

ReMatch:

A table with a painting of a city and a vase of flowers.

Figure 9. Comparison of image captioning performance between our method, original backbone and prior embedding approaches (all based on Qwen2-VL-2B). Part 2.



Top5 results (Ours)

- 1. pier
- 2. boathouse
- 3. bridge
- 4. cottage
- 5. Chalet

Top5 results (VLM2Vec-V2)

- 1. boathouse
- 2. pier
- 3. boardwalk
- 4. creek
- 5. bridge

GT: pier



Top5 results (Ours)

- 1. desk lamp
- 2. lampshade
- 3. portable heater
- 4. candle
- 5. Vase

Top5 results (VLM2Vec-V2)

- 1. lampshade
- 2. desk lamp
- 3. candle
- 4. portable heater
- 5. Lipstick

GT: desk lamp

Figure 10. Comparison of classification performance between ReMatch and the baseline.



Top5 results (Ours)

- 1. The fence is green
- 2. The fence is gray
- 3. The bench is brown
- 4. The giraffe is brown
- 5. The grass is tan

Top5 results (VLM2Vec-V2)

- 1. The fence is gray
- 2. The fence is green
- 3. The bench is brown
- 4. The shirt is brown
- 5. The giraffe is brown

What is the color of the fence made of metal? GT: The fence is green



Top5 results (Ours)

- 1. off
- 2. out
- 3. not a question
- 4. ok
- 5. They

Top5 results (VLM2Vec-V2)

- 1. oui
- 2. ck
- 3. z
- 4. what
- 5. Today

Are these switches on or off? GT: off

Figure 11. Comparison of visual question answering performance between ReMatch and the baseline.

Top3 results (Ours) Top3 results (Ours) Top3 results (VLM2Vec-V2) Top3 results (VLM2Vec-V2) Top3 results (VLM2Vec-V2) Top3 results (VLM2Vec-V2)

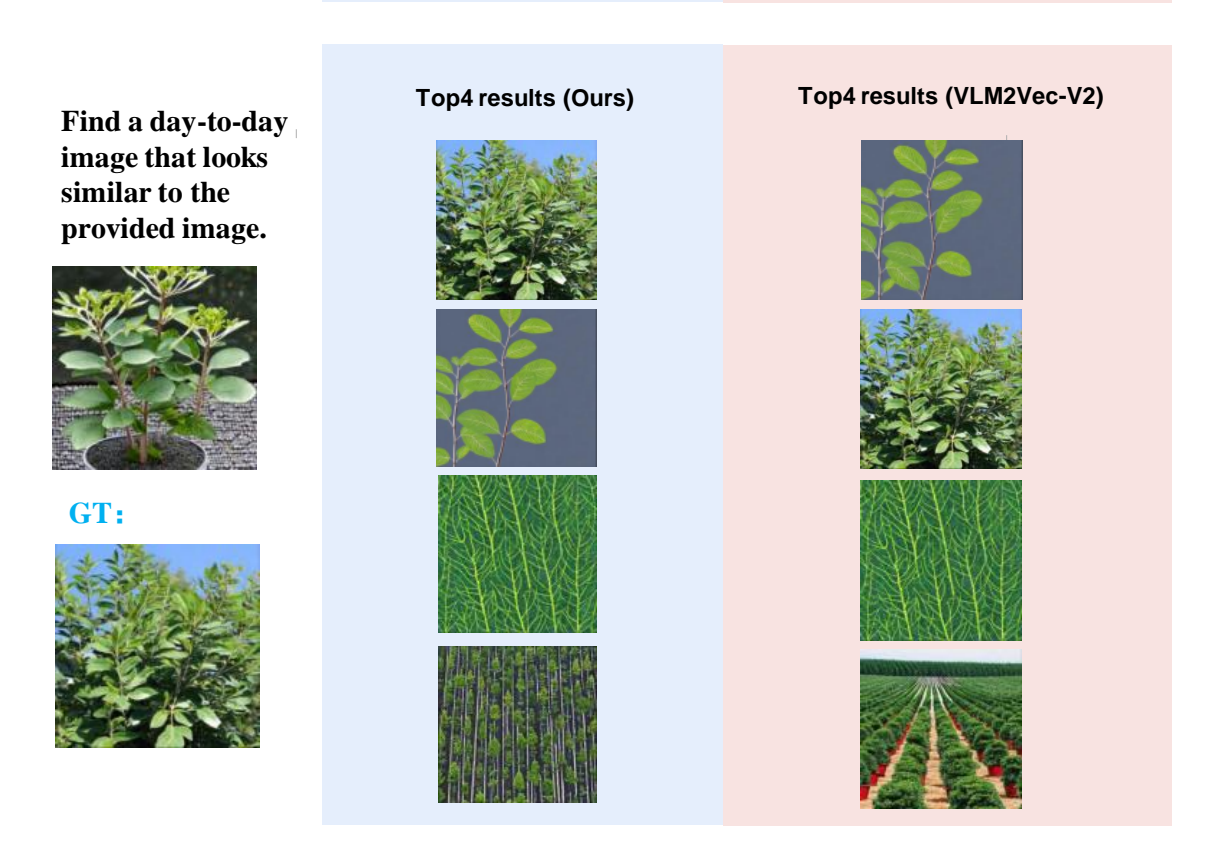


Figure 12. Comparison of retrieval performance between ReMatch and the baseline. Confidence-ordered from top to bottom (highest to lowest).

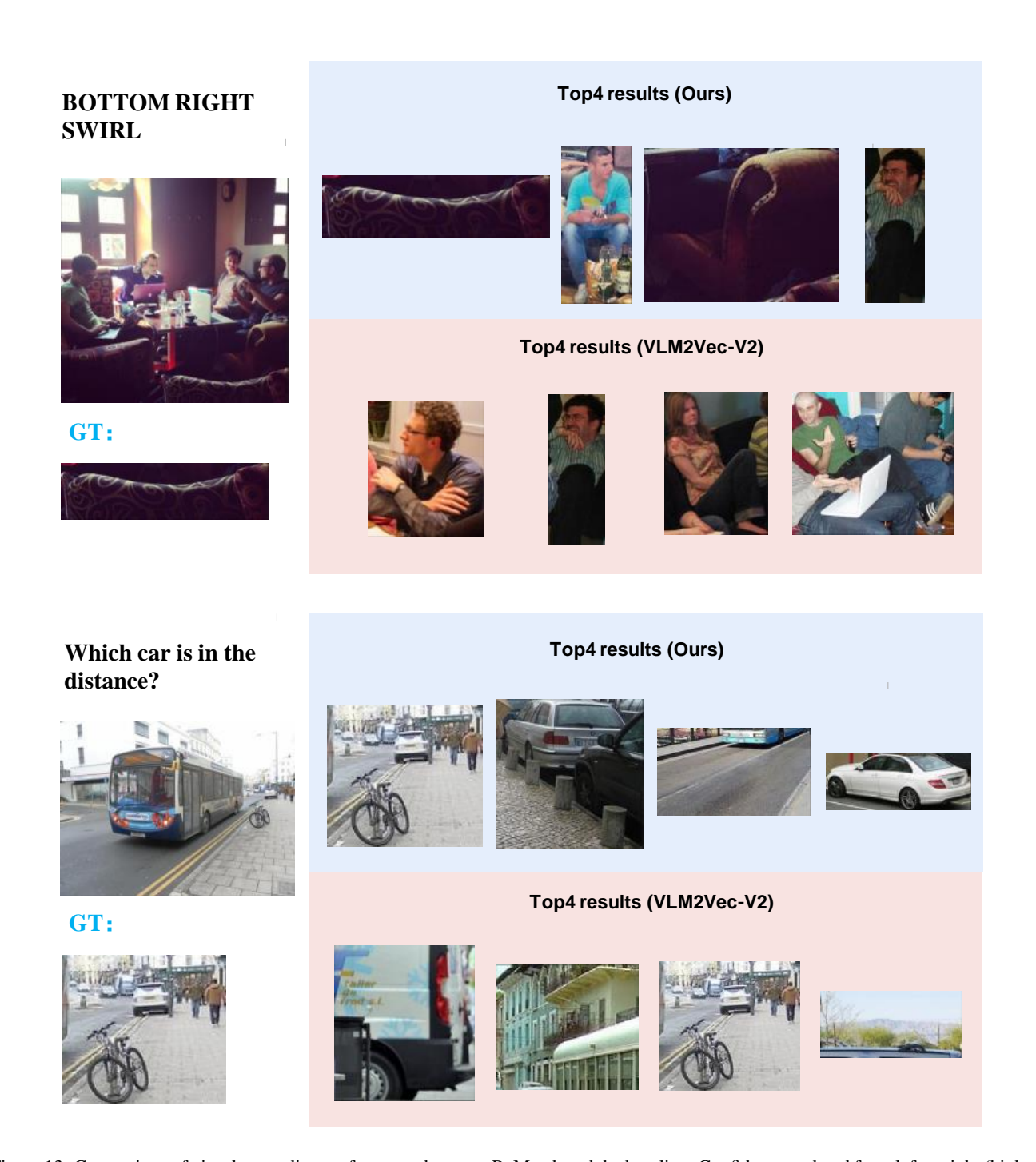


Figure 13. Comparison of visual grounding performance between ReMatch and the baseline. Confidence-ordered from left to right (highest to lowest).